Effect of the Breit interaction on K x-ray hypersatellite spectra

Mau Hsiung Chen and Bernd Crasemann
Department of Physics and Chemical Physics Institute, University of Oregon, Eugene, Oregon 97403

Hans Mark*
Department of the Air Force, Washington, D. C. 20330
(Received 29 June 1981)

The Breit interaction is found to substantially affect predicted multiplet splittings of double-inner-shell-vacancy configurations in heavy atoms. Not only can the magnitude of the splitting be greatly changed in some cases but the level order can also be altered with respect to that predicted from the Coulomb interaction alone. Inclusion of the full Breit interaction in the splitting of $[KL]$ hole states reduces the $K\alpha_1$ x-ray hypersatellite shift by ~ 10 eV and increases the $K\alpha_2^h$ shift by ~ 16 eV at $Z=80$; the intensity ratio of $K\alpha_1^h$ to $K\alpha_2^h$ is reduced by $\sim 25\%$ at $Z=18$ and increased by $\sim 7\%$ at $Z=60$.

I. INTRODUCTION

Relativistic treatments of atomic structure and transitions are currently receiving renewed attention because of their importance for the analysis of complex x-ray spectra from multiply ionized atoms that can occur in high-temperature plasmas[1] or be generated in heavy-ion-atom collisions.[2] One factor that has not been thoroughly analyzed in this context is the effect of the Breit energy, which arises from the interaction between any two atomic electrons due to the exchange of a single transverse photon.

In most recent relativistic calculations of binding and x-ray transition energies in heavy atoms with one[3-7] and two[8-11] inner-shell vacancies, the Breit operator is expressed in a form which is valid only in the long-wavelength limit, viz.,

$$H_{\mathrm{Br}}=-\frac{1}{2r_{12}}\left[\vec{\alpha}_1\cdot\vec{\alpha}_2+\frac{(\vec{\alpha}_1\cdot\vec{r}_{12})(\vec{\alpha}_2\cdot\vec{r}_{12})}{r_{12}^2}\right], \quad (1)$$

where the $\vec{\alpha}_i$ are Dirac matrices and r_{12} is the distance between the two interacting electrons. In most of those calculations dealing with double-inner-shell-hole states,[8-11] only the configuration-average contribution of this Breit operator is taken into account.

Currently there is much interest in a particular kind of atomic inner-shell double-hole states, viz., states in which the K shell is entirely empty. The radiative deexcitation of such $[1s^2]$ states through one-electron transitions gives rise to so-called K x-ray *hypersatellites* ($K\alpha_{1,2}^h$, $K\beta^h$, $\cdots$). The only calculations involving double-hole states that include the Breit interaction in the splitting calculations[12-14] pertain to the $K\alpha$ hypersatellite energies of the two elements Hg and Tm. There exists no systematic study of K hypersatellite energies that includes the effect of the Breit interaction on the multiplet splitting.

The $K\alpha_{1,2}$ hypersatellite intensity ratio has recently been analyzed by Åberg *et al.*[11,15] in terms of the intermediate coupling scheme. In these intermediate-coupling calculations, the energy matrix contained only the electrostatic interaction; the contribution of the Breit interaction was neglected in determining the mixing coefficients. Furthermore, the differences between the $K\alpha_1^h$ and $K\alpha_2^h$ x-ray energies and matrix elements were neglected. These differences, arising from relativity, are the dominant factors which reduce the intensity ratios of $K\alpha_1^h$ to $K\alpha_2^h$ from their $j-j$ coupling limit.

Here we report on a systematic study of the effect that the Breit operator, in a more accurate form, has on the multiplet splitting of states with two inner-shell vacancies. We apply the calculation to the shift of $K\alpha$ and $K\beta$ x-ray hypersatellites. We also calculate the x-ray emission rates of the double-K-hole states, using Dirac-Hartree-Slater (DHS) wave functions. We then use the x-ray matrix elements to calculate the intensity ratios of $K\alpha_1^h$ to $K\alpha_2^h$ and $K\beta_1^h$ to $K\beta_3^h$ in intermediate coupling, with and without the Breit interaction being included in the energy matrix, in order to in-

vestigate the effect that the Breit interaction has on these intensity ratios.

II. THEORY

In our previous relativistic calculations of atomic-energy levels,[7] we computed the configuration-average total energy as the expectation of the total Hamiltonian, consisting of kinetic energy, electrostatic interaction, Breit interaction, and vacuum polarization. The nucleus was taken to be a homogeneously charged sphere of radius $R=1.20\times10^{-13}A^{1/3}$ cm, where A is the mass number. The Breit interaction was expressed in the long-wavelength approximation [Eq. (1)].

The nuclear charge distribution has a noticeable effect on inner-shell-level energies. For example, a Fermi distribution causes the $1s$ level at $Z=95$ to be 6 eV more tightly bound than a uniformly charged sphere. In the present work, we therefore use the two-parameter Fermi model for the nuclear charge distribution

$$\rho(r)=\frac{\rho_0}{1+e^{(r-c)/a}} . \tag{2}$$

The half-density radius c and skin-thickness parameter a are taken from high-energy electron scattering results[16]

$$c=(2.2291A^{1/3}-0.906\ 76)\times10^{-5}\ \text{a.u.} ,$$
$$a=1.039\times10^{-5}\ \text{a.u.}$$

Instead of the long-wavelength-limit Breit operator [Eq. (1)] employed in earlier work,[3–11] we use a more exact form of the Breit interaction, appropriate in the local approximation[17]

$$H_{\rm Br}=-\frac{1}{r_{12}}[\vec{\alpha}_1\cdot\vec{\alpha}_2\cos\omega r_{12}+(1-\cos\omega r_{12})] . \tag{3}$$

Here, ω is the energy transferred by the virtual photon. From Eq. (3) we calculate the configuration-average contribution from the Breit interaction.

For atoms with double inner-shell vacancies, the multiplet splitting can be found by evaluating the corresponding coupled-two-hole matrix elements of the electrostatic and Breit interaction operators. Because closed shells do not contribute to the multiplet splitting,[18] the splitting of the double-hole states is determined by the coupled-two-hole states alone. The sum of the electrostatic and Breit operators is

$$H_{\rm CBr}=\frac{1-\vec{\alpha}_1\cdot\vec{\alpha}_2}{r_{12}}\cos\omega r_{12} . \tag{4}$$

Hence, the energy matrix of the electrostatic and Breit operators between the antisymmetrized j-j-coupled two-hole states, which can be separated into direct and exchange matrix elements, is

$$\langle j_1j_2JM\,|\,r_{12}^{-1}(1-\vec{\alpha}_1\cdot\vec{\alpha}_2)\cos\omega r_{12}\,|\,j_1j_2JM\rangle = D-E . \tag{5}$$

The matrix element of $H_{\rm CBr}$ [Eq. (5)] is a special case of Eqs. (11) and (19) of our earlier work,[19] viz.,

$$D=\sum_{\lambda=0}^{\infty}(-1)^{1+J}(2j_1+1)(2j_2+1)\begin{Bmatrix} j_1 & j_2 & J\\ j_2 & j_1 & \lambda\end{Bmatrix}\begin{pmatrix} j_1 & j_1 & \lambda\\ -\frac{1}{2} & \frac{1}{2} & 0\end{pmatrix}\begin{pmatrix} j_2 & j_2 & \lambda\\ -\frac{1}{2} & \frac{1}{2} & 0\end{pmatrix}$$
$$\times\left[\left[\langle W_{11}\gamma_\lambda W_{22}\rangle+\frac{\lambda}{2\lambda-1}\langle V_{11}\gamma_{\lambda-1}V_{22}\rangle+\frac{\lambda+1}{2\lambda+3}\langle V_{11}\gamma_{\lambda+1}V_{22}\rangle\right]\right.$$
$$\left.\times\prod(l_1\lambda l_1)-(1-\delta_{\lambda0})\frac{4\kappa_1\kappa_2}{\lambda(\lambda+1)}\langle U_{11}\gamma_\lambda U_{22}\rangle\prod(l_1\ \lambda+1\ l_1)\right] \tag{6}$$

and

$$E=\sum_{\lambda=0}^{\infty}(2j_1+1)(2j_2+1)\begin{Bmatrix} j_1 & j_2 & J\\ j_1 & j_2 & \lambda\end{Bmatrix}\begin{pmatrix} j_1 & j_2 & \lambda\\ -\frac{1}{2} & \frac{1}{2} & 0\end{pmatrix}^2$$
$$\times\left[\left[\langle W_{12}\gamma_\lambda W_{21}\rangle+\frac{\lambda}{2\lambda-1}\langle P^\lambda_{12}\gamma_{\lambda-1}P^\lambda_{21}\rangle+\frac{\lambda+1}{2\lambda+3}\langle Q^\lambda_{12}\gamma_{\lambda+1}Q^\lambda_{21}\rangle\right]\prod(l_1\lambda l_2)\right.$$
$$\left.-(1-\delta_{\lambda0})\frac{(\kappa_1+\kappa_2)^2}{\lambda(\lambda+1)}\langle U_{12}\gamma_\lambda U_{21}\rangle\prod(l_1\ \lambda+1\ l_2)\right] , \tag{7}$$

where

$$\langle X_{i'j'}\gamma_\lambda X_{ij}\rangle = \int_0^\infty \int_0^\infty X_{i'j'}(r_1)\gamma_\lambda(r_1 r_2) \times X_{ij}(r_2)dr_1 dr_2 , \quad (8)$$

$$W_{ij}(r)=G_j(r)G_j(r)+F_i(r)F_j(r) , \quad (9)$$

$$P_{ij}^\lambda(r)=\lambda^{-1}(\kappa_j-\kappa_i)U_{ij}(r)+V_{ij}(r) , \quad (10)$$

$$Q_{ij}^\lambda(r)=(\lambda+1)^{-1}(\kappa_j-\kappa_i)U_{ij}(r)-V_{ij}(r) , \quad (11)$$

$$U_{ij}(r)=G_i(r)F_j(r)+F_i(r)G_j(r) , \quad (12)$$

$$V_{ij}(r)=G_i(r)F_j(r)-F_i(r)G_j(r) , \quad (13)$$

and

$$\prod(l_1\lambda l_2)=\begin{cases}1 & \text{if } l_1+\lambda+l_2 \text{ is even}\\ 0 & \text{otherwise}\end{cases} . \quad (14)$$

We have

$$\gamma_\lambda(r_1 r_2)=-(2\lambda+1)\omega j_\lambda(\omega r_<)\mathscr{Y}_\lambda(\omega r_>) , \quad (15)$$

where $r_<$ ($r_>$) is the smaller (larger) of r_1 and r_2; j_λ and $\mathscr{Y}_\lambda$ are spherical Bessel functions of the first and second order, respectively. Further details are provided in Ref. 19.

The splitting of the double-hole states is found by subtracting the j-j average Coulomb-plus-Breit energy of the pertinent two-hole configuration from the energies, given by Eq. (5), of the coupled-two-hole states. The mixing between $[KL_2]J=1$ and $[KL_3]J=1$, and between $[KM_2]J=1$ and $[KM_3]J=1$, is then included by configuration interaction. The needed energy matrices are found by the procedure described above. In order to study the effect of the Breit interaction on the $K\alpha_{1,2}$ hypersatellite intensity ratio, the mixing calculations are carried out twice, with and without the contribution of the Breit interaction being included in the energy matrix.

The double-hole-state relativistic x-ray emission rates are calculated in j-j coupling, with a single potential corresponding to the initial double-K-hole state, following the usual procedure.[20,21] The eigenfunctions with the mixing coefficients obtained in the diagonalization are then incorporated in the x-ray matrix elements to calculate the $K\alpha^h$ and $K\beta^h$ intensity ratios.

III. RESULTS AND DISCUSSION

A. Dirac-Hartree-Slater vs Dirac-Fock energies

We use a local approximation to the atomic potential and find zeroth-order wave functions by minimizing the average energy of the corresponding j-j configurations. These zeroth-order wave functions are then used to perform perturbation calculations. Electric energies (Dirac-Fock energies) and Breit-interaction energies (including transverse correction) for $_{80}$Hg from the present DHS model are compared in Table I with results from multiconfigurational Dirac-Fock (MCDF) calculations.[14] Our DHS results are seen to agree exceedingly well with the results of MCDF calculations; clearly the DHS model can be relied upon, for all practical purposes, to produce results of adequate accuracy.

B. Multiplet splitting

On the basis of the foregoing theory, we have calculated the splitting of j-j coupled KL, LL, LM, and other double-hole states of a number of elements between $Z=65$ and 95. This work was performed in connection with the preparation of tables of L x-ray satellite energies.[22]

The effect of the Breit interaction on the multiplet splitting of most double-hole states is found to be quite significant. The effect is striking, for example, in the case of the $J=0$ and 1 multiplet states of the $[1s2p_{1/2}]$ two-hole configuration (Fig. 1). Not only does the Breit energy enhance this splitting by as much as a factor of 3 at high Z, but it reverses the level order. Other examples of the Breit-interaction effect on multiplet splittings are shown in Figs. 2 and 3.

TABLE I. Electric (Dirac-Fock) and Breit-interaction energies (in eV) of Hg-atom hole states, as calculated from a multiconfigurational Dirac-Fock (MCDF) approach[a] and from the present Dirac-Hartree-Slater (DHS) model.

	$E(1s)$		$E(2p_{3/2})$		$E(1s^2)$		$E(1s2p_{3/2};J=1)$	
	MCDF	DHS	MCDF	DHS	MCDF	DHS	MCDF	DHS
Electric	−451 116.1	−451 116.3	−522 347.8	−522 349.3	−366 177.7	−366 177.0	−438 400.4	−438 400.7
Breit	306.0	306.2	570.4	570.3	206.1	206.1	283.4	283.3

[a]Reference 14.

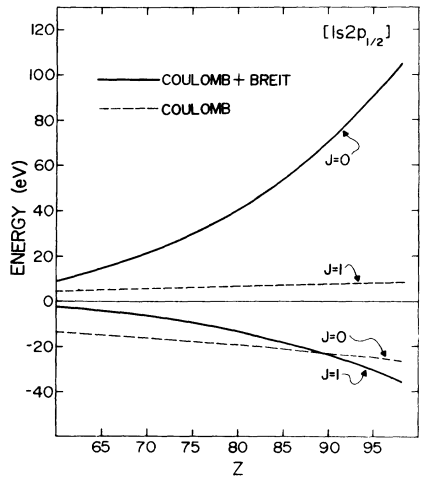

FIG. 1. Fine-structure splitting between the $J=0$ and 1 multiplet states of the $[1s2p_{1/2}]$ two-hole configuration, as a function of atomic number Z. Inclusion of the Breit interaction in addition to the Coulomb interaction (solid curve) causes the splitting to increase greatly at high Z, and *inverts the order* of the $J=0$ and 1 levels.

reverses the level order. Other examples of the Breit-interaction effect on multiplet splittings are shown in Figs. 2 and 3.

The importance of the magnetic interaction in the multiplet splitting of Li-like ions of low-Z atoms has previously been found.[23] In this earlier work,[23] the long-wavelength limit of the magnetic

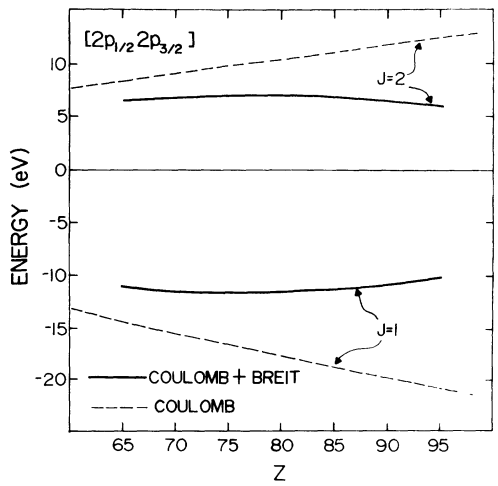

FIG. 2. Multiplet splitting between the $J=1$ and 2 levels of the $[2p_{1/2}2p_{3/2}]$ double-hole state, as a function of atomic number. Splitting computed with the Coulomb interaction (broken curves) is reduced when the Breit interaction is included in the calculation (solid curves).

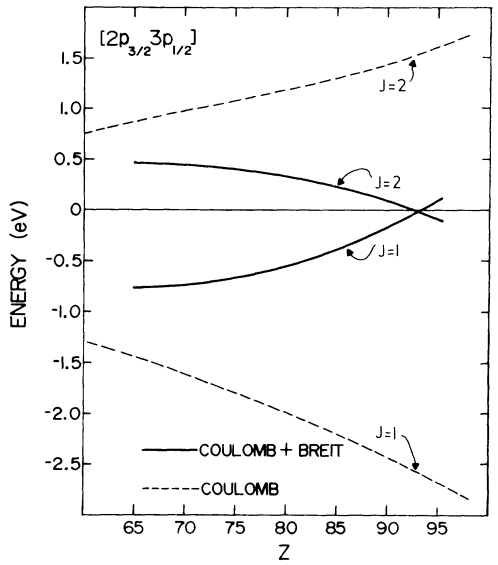

FIG. 3. Splitting between the $J=1$ and 2 multiplet states of the $[2p_{3/2}3p_{1/2}]$ two-hole configuration, as a function of atomic number Z. A calculation with the Coulomb interaction alone (broken curves) shows splitting that increases with Z. When the Breit interaction is included in the calculation (solid curves), splitting is predicted to decrease with increasing atomic numbers, and the level order is inverted above $Z=93$.

interaction was used and a retardation correction was not included in the splitting calculations. These approximations are good for low-Z atoms, but they are not adequate for heavy elements[17] as considered here.

C. $K\alpha$ and $K\beta$ hypersatellite energies

Experimental data exist, in particular, for the $K\alpha$ hypersatellites $K\alpha_1^h$ and $K\alpha_2^h$, which arise from the double-hole-state transitions $[1s^2]\rightarrow[1s2p_{3/2}]$ and $[1s^2]\rightarrow[1s2p_{1/2}]$, respectively.[24] The energy shift of these $K\alpha$ hypersatellites with respect to the diagram lines has been calculated by several groups,[9–14] mostly without, however, including the splitting of the final $[KL]$ double-hole state due to the Breit interaction. Moreover, the configuration-average Breit energy was calculated in the long-wavelength approximation [Eq. (1)].

We have applied the theory outlined in Sec. II to compute the energy shift of the $K\alpha$ and $K\beta$ hypersatellites in intermediate coupling, including the full Breit interaction [Eq. (3)] and the final-state splitting produced by the Coulomb and Breit interactions. The $K\alpha_{1,2}^h$ and $K\beta_{1,3}^h$ energies were

determined by performing separate relativistic self-consistent-field calculations for the intitial $[KK]$ and final $[KL]$ or $[KM]$ double-hole states to find the configuration-average transition energies. The splitting of the final $[KL]$ and $[KM]$ states was then calculated by the procedure described in Sec. II. The $K\alpha$ and $K\beta$ diagram-line energies were calculated according to the same model, i.e., with a Fermi nuclear charge distribution and the full Breit interaction.[25]

We neglect the self-energy contribution to the hypersatellite shifts. This contribution has never been calculated *ab initio* but is estimated to be rather small (~ 2 eV at $Z=80$).[8] We also omit contributions due to electron correlation. The Breit-energy contribution to the $K\alpha_1^h - K\alpha_1$ hypersatellite energy shift increases from 2.7% at $Z=30$ to 21.7% at $Z=95$, and the Breit contribution to the $K\beta_1^h - K\beta_1$ energy shift ranges from 2.1% at $Z=30$ to 9.4% at $Z=65$ as illustrated in Fig. 4.

The mixing between $[KL_2]J=1$ and $[KL_3]J=1$ final states is found to contribute significantly to the hypersatellite energy shifts for light elements (~ 6 eV at $Z=20$), but less at medium Z (~ 0.8 eV at $Z=54$); for heavy elements, this contribution is negligible (~ 0.1 eV at $Z=80$). Mixing between these two $J=1$ states is reduced if the Breit energy is included in the energy matrix for the intermediate-coupling calculation. Since all the MCDF computations[11-13] fail to include the Breit energy in the mixing calculations, they tend to overestimate the energy shift due to configuration interaction between these two $J=1$ states.

The calculated $K\alpha$ and $K\beta$ hypersatellite energy shifts are listed in Table II. Inclusion of the Breit interaction in the splitting calculation of $[KL]$ hole states reduces the $K\alpha_1$ hypersatellite energy by ~ 10 eV and increases the $K\alpha_2^h$ shift by ~ 16 eV at $Z=80$. Our calculated $K\alpha_1^h$ shift for Hg (1177.4 eV) agrees very well with the result (1176.8 eV) from a MCDF computation[14] which also included the full Breit interaction in the splitting calculations.

In Figs. 5 and 6, we compare calculated and measured[9-10,26-31] $K\alpha_{1,2}$ hypersatellite energy shifts. For $Z<36$, present results differ by less than 2 eV from those of MCDF computations in which the Breit interaction was omitted from the splitting calculations.[11] The experimental energies are not sufficiently accurate to differentiate between the theoretical predictions. Agreement between experiment and theory is good within the uncertainties, however, except for one measurement[10] at $Z=80$.

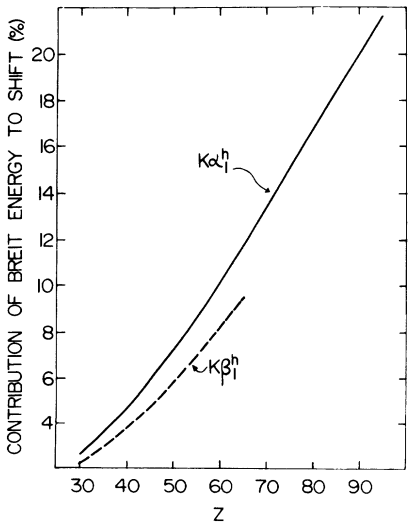

FIG. 4. Contribution (in percent) of the Breit energy to the energy shifts of $K\alpha_1$ and $K\beta_1$ hypersatellites with reference to the respective diagram lines.

TABLE II. Calculated energy shifts (in eV) of the $K\alpha_{1,2}^h$ hypersatellites with respect to the $K\alpha_{1,2}$ diagram lines, and the $K\beta_{1,3}^h$ hypersatellites with respect to the $K\beta_{1,3}$ diagram lines.

Atomic number	$K\alpha_1^h - K\alpha_1$	$K\alpha_2^h - K\alpha_2$	$K\beta_1^h - K\beta_1$	$K\beta_3^h - K\beta_3$
18	184.4	175.5	226.3	225.4
20	206.3	197.4	255.5	254.3
25	260.7	254.9	324.8	324.5
30	317.3	314.0	397.4	397.0
36	388.0	387.6	492.3	492.1
40	438.9	439.1	558.8	558.6
45	506.6	506.4	645.7	645.2
47	535.0	534.3	681.8	681.2
49	564.1	562.7	718.8	718.0
54	641.1	636.9	815.5	814.0
60	742.9	733.1	941.7	938.7
65	836.1	819.8	1055.6	1051.1
70	940.0	913.2		
74	1029.2	993.2		
78	1125.7	1078.8		
80	1177.4	1123.9		
85	1316.5	1243.7		
88	1408.2	1321.6		
90	1473.0	1376.0		
92	1541.5	1432.7		
95	1650.7	1522.6		

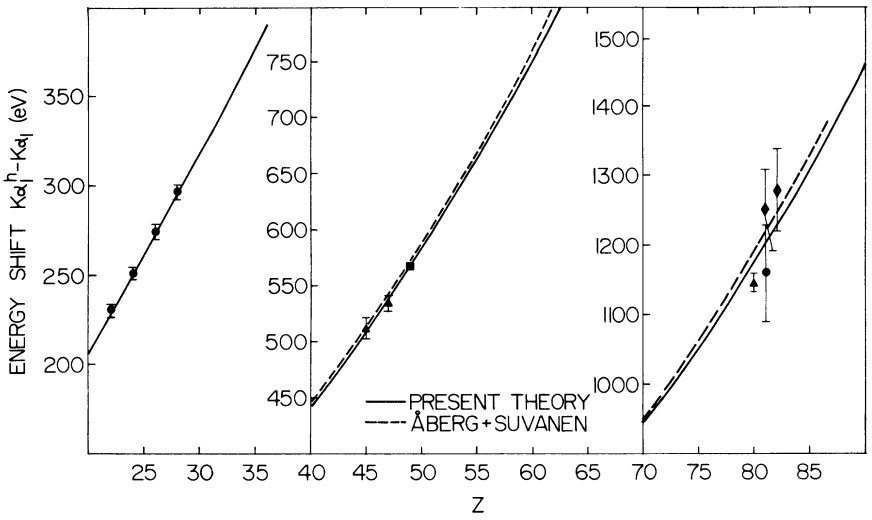

FIG. 5. Calculated shift of the $K\alpha_1$ x-ray hypersatellite with respect to the diagram line, as a function of atomic number Z (solid curve). For comparison, predictions due to Åberg and Suvanen (Ref. 11) are shown (broken curve), as well as experimental results from the following sources: (a) $20<Z<40$, Ref. 27; (b) $40<Z<70$, Refs. 30 (triangles) and 31 (square); (c) $70<Z<90$, Refs. 9 (dot), 10 (triangle), and 29 (diamonds).

The calculated $K\beta_{1,3}$ energy shifts are compared with experiment[26,29] in Fig. 7. Agreement is fair at $Z=25$ and 31, but the measured energy shift for $Z=49$ far exceeds the theoretical prediction.

D. $K\alpha^h$ and $K\beta^h$ intensity ratios

The x-ray emission rates for double-hole states were calculated with DHS wave functions as indicated in Sec. II.[20,21] Radiative rates for transitions from p states are listed in Table III. The K x-ray emission rates, per K hole, are larger for double-

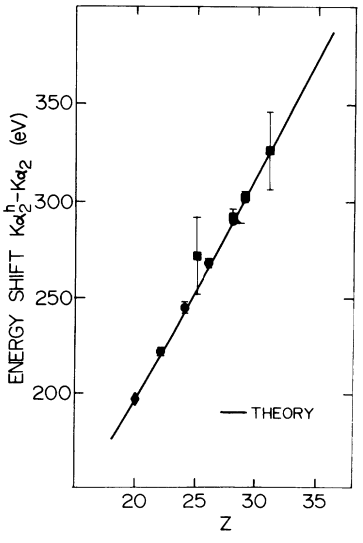

FIG. 6. Calculated shift of the $K\alpha_2$ x-ray hypersatellite with respect to the diagram line, as a function of atomic number Z. For comparison, experimental results are shown from Refs. 26 (squares), 27 (dots), and 28 (diamond).

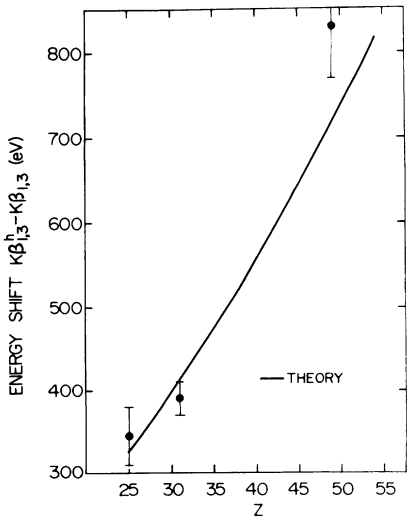

FIG. 7. Calculated shift of the $K\beta_{1,3}$ x-ray hypersatellites with respect to the diagram lines, as a function of atomic number Z. For comparison, experimental data from Refs. 26 and 29 are also shown.

TABLE III. X-ray transition rates (in a.u.[a]) from $[1s^2]$ double-K-hole states.[b]

Atomic number	Final hole state $[1s2p]$	$[1s3p]$	$[1s4p]$	$[1s5p]$	Total rate
18	6.577(−3)	6.824(−4)			7.259(−3)
20	1.035(−3)	1.258(−3)			1.161(−2)
25	2.682(−2)	3.363(−3)			3.018(−2)
30	5.776(−2)	7.323(−3)			6.510(−2)
36	1.232(−1)	1.774(−2)	2.023(−3)		1.430(−1)
40	1.905(−1)	2.936(−2)	4.431(−3)		2.244(−1)
45	3.094(−1)	5.088(−2)	8.587(−3)		3.692(−1)
47	3.698(−1)	6.214(−2)	1.085(−3)		4.433(−1)
49	4.387(−1)	7.520(−2)	1.387(−3)	2.370(−4)	5.286(−1)
54	6.522(−1)	1.168(−1)	2.417(−2)	3.347(−3)	7.977(−1)
60	1.002	1.871(−1)	4.105(−2)	6.430(−3)	1.239
70	1.869	3.672(−1)	8.242(−2)	1.124(−2)	2.337
80	3.186	6.475(−1)	1.549(−1)	2.888(−2)	4.038
85	4.050	8.337(−1)	2.059(−1)	4.404(−2)	5.170
90	5.069	1.055	2.682(−1)	6.381(−2)	6.514
95	6.255	1.310	3.423(−1)	8.592(−2)	8.079

[a]1 a.u. = 27.21 eV/$\hbar$ = 4.134×10^{17} s^{-1}.
[b]Numbers in parentheses signify powers of ten, e.g., 6.577(−3) = 6.577×10^{-3}.

hole states than for single-hole states (by ~38% at $Z=18$ and by ~9% at $Z=60$).

Table IV contains $K\alpha_1^h$ to $K\alpha_2^h$ and $K\beta_1^h$ to $K\beta_3^h$ intensity ratios from the present calculations in intermediate coupling, including the effect of the Breit interaction and of the differences in x-ray matrix elements. The $K\alpha^h$ intensity ratios are compared in Fig. 8 with the results of MCDF calculations[11] and with experiment.[15,26,27,31,32]

For low-Z elements, the $K\alpha_1^h$ x-ray transition

TABLE IV. Theoretical hypersatellite intensity ratios.

Atomic number	$I(K\alpha_1^h)/I(K\alpha_2^h)$	$I(K\beta_1^h)/I(K\beta_3^h)$
18	0.013	0.0093
20	0.023	0.022
25	0.169	1.09
30	0.358	0.389
36	0.772	0.831
40	1.04	1.10
45	1.27	1.34
47	1.34	1.42
49	1.40	1.48
54	1.52	1.61
60	1.60	1.72
65	1.64	1.78
70	1.66	
74	1.66	
80	1.64	
85	1.62	
90	1.59	
95	1.56	

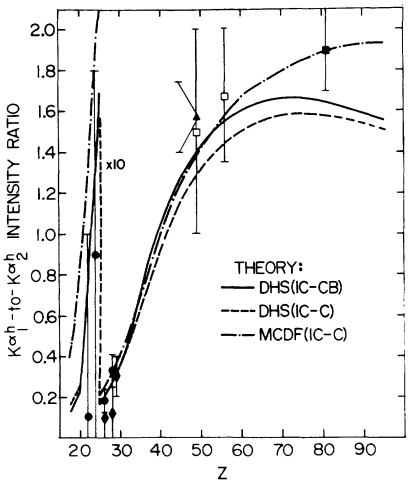

FIG. 8. The $K\alpha_1^h$-to-$K\alpha_2^h$ x-ray hypersatellite intensity ratio, as a function of atomic number Z. Theoretical predictions are from the present DHS computations including Coulomb and Breit energies in the intermediate-coupling calculations (solid curve) and including only the Coulomb energy in the intermediate-coupling calculations (broken curve), and from the MCDF computations of Åberg and Suvanen (Ref. 11) (dot-dash curve).

$[1s^2] \rightarrow [1s\,2p]^3P_1$ is dipole forbidden in LS coupling. X-ray emission then arises from mixing between $^3P_1$ and $^1P_1$ of the final $[1s\,2p]$ configuration. The $K\alpha_1^h$-to-$K\alpha_2^h$ intensity ratio for low-Z atoms is therefore quite sensitive to the atomic model. Including the Breit interaction in the intermediate-coupling calculations reduces the mixing between $[KL_2]J=1$ and $[KL_3]J=1$ states, which in turn decreases the $K\alpha_1^h$-to-$K\alpha_2^h$ intensity ratio at low Z ($\sim 25\%$ at $Z=18$) and increases this intensity ratio for medium and heavier elements ($\sim 7\%$ at $Z=60$). Since relativity affects the $2p_{1/2}$ level much more than the $2p_{3/2}$ level of heavy elements, the $K\alpha^h$ intensity ratio does not increase monotonically toward the j-j coupling limit of 2. Instead, the $K\alpha$ hypersatellite intensity ratio reaches a maximum at $Z \cong 70$ and then decreases with increasing Z. At high atomic numbers ($Z > 70$), the ordinary $K\alpha_1$-to-$K\alpha_2$ x-ray intensity ratio follows a similar trend.[20]

The differences between our present hypersatellite intensity ratios and those from MCDF calculations[11] at low Z are partly due to the differences in wave functions, and partly to the fact that we include the Breit interaction in the mixing calculations. The discrepancy between the theoretical intensity ratios at high Z is mainly due to the fact that the difference between the $K\alpha_1^h$ and $K\alpha_2^h$ x-ray matrix elements was neglected in the MCDF calculations.[11] Experimental hypersatellite intensity ratios are not sufficiently accurate in the medium- and low-Z region to differentiate between the calculations, and only one experimental ratio is available for a heavy element. Additional, accurate hypersatellite intensity-ratio measurements are very much needed.

ACKNOWLEDGMENTS

We are indebted to Teijo Åberg for constructive comments and for providing detailed results of some of his own computations. We thank J. P. Desclaux and C. W. E. van Eijk for helpful correspondence. This work was supported in part by the U.S. Air Force Office of Scientific Research through Grant No. AFOSR-79-0026.

---

*Present address: National Aeronautics and Space Administration, Code AD, Washington D.C. 20546.

[1]R. L. Kauffman and P. Richard, in *Methods of Experimental Physics 13A,* edited by D. Williams (Academic, New York, 1976), p. 148.

[2]I. A. Sellin, *Structure and Collisions of Ions and Atoms* (Springer, Berlin, 1978).

[3]A. M. Desiderio and W. R. Johnson, Phys. Rev. A 3, 1267 (1971).

[4]B. Fricke, J. P. Desclaux, and J. T. Waber, Phys. Rev. Lett. 28, 714 (1972).

[5]K. T. Cheng and W. R. Johnson, Phys. Rev. A 14, 1943 (1976).

[6]T. A. Carlson and C. W. Nestor, Jr., At. Data Nucl. Data Tables 19, 153 (1977).

[7]K. -N. Huang, M. Aoyagi, M. H. Chen, B. Crasemann, and H. Mark, At. Data Nucl. Data Tables 18, 243 (1976).

[8]M. H. Chen, B. Crasemann, K. -N. Huang, M. Aoyagi, and H. Mark, At. Data Nucl. Data Tables 19, 97 (1977).

[9]J. P. Desclaux, Ch. Briançon, J. P. Thibaud, and R. J. Walen, Phys. Rev. Lett. 32, 447 (1974).

[10]K. Schreckenbach, H. G. Börner, and J. P. Desclaux, Phys. Lett. A 63, 330 (1977).

[11]T. Åberg and M. Suvanen, in *Advances in X-Ray Spectroscopy,* edited by C. Bonnelle and C. Monde (Pergamon, New York 1980).

[12]J. P. Desclaux, Phys. Scr. 21, 436 (1980).

[13]N. Beatham, I. P. Grant, B. J. McKenzie, and S. J. Rose, Phys. Scr. 21, 423 (1980).

[14]I. P. Grant and B. J. McKenzie, J. Phys. B 13, 2671 (1980).

[15]T. Åberg, J. P. Briand, P. Chevallier, A. Chetioui, and J. P. Rozet, J. Phys. B 9, 2815 (1976).

[16]H. R. Collard, L. R. B. Elton, and R. Hofstadter, in *Landolt-Börnstein, Numerical Data and Functional Relationships in Science and Technology* (Springer, Berlin, 1967), Group I, Vol. 2.

[17]J. B. Mann and W. R. Johnson, Phys. Rev. A 4, 41 (1971).

[18]J. C. Slater, *Quantum Theory of Atomic Structure* (McGraw-Hill, New York, 1960), Vol. I.

[19]M. H. Chen, E. Laiman, B. Crasemann, M. Aoyagi, and H. Mark, Phys. Rev. A 19, 2253 (1979).

[20]J. H. Scofield, in *Atomic Inner-Shell Processes,* edited by B. Crasemann (Academic, New York, 1975), Vol. 1, p. 265; Phys. Rev. 179, 9 (1969); Phys. Rev. A 9, 1041 (1974).

[21]M. H. Chen, B. Crasemann, and H. Mark (unpublished).

[22]F. Parente, M. H. Chen, B. Crasemann, and H. Mark, At. Data Nucl. Data Tables (in press).

[23]K. J. Cheng, J. P. Desclaux, and Y. K. Kim, J. Phys.

B 11, L359 (1978).
[24]J. P. Briand, P. Chevallier, M. Tavernier, and J. P. Rozet, Phys. Rev. Lett. 27, 777 (1971).
[25]M. H. Chen, B. Crasemann, M. Aoyagi, K. -N. Huang, and H. Mark, At. Data Nucl. Data Tables (in press).
[26]J. P. Briand, A. Touati, M. Frilley, P. Chevallier, A. Johnson, J. P. Rozet, M. Tavernier, S. Shafroth, and M. O. Krause, J. Phys. B 9, 1055 (1976).
[27]J. Ahopelto, E. Rantavuori, and O. Keski-Rahkonen, Phys. Scr. 20, 71 (1979).
[28]P. Richard, Phys. Fenn. 9, S1, 3 (1974).
[29]J. P. Briand, P. Chevallier, A. Johnson, J. P. Rozet, M. Tavernier, and A. Touati, Phys. Lett. 49A, 51 (1974).
[30]C. W. E. van Eijk, J. Wijnhorst, and M. A. Popelier, Phys. Rev. A 20, 1749 (1979).
[31]C. W. E. van Eijk, J. Wijnhorst, and M. A. Popelier, Phys. Rev. A 24, 854 (1981).
[32]J. P. Briand, P. Chevallier, A. Johnson, J. P. Rozet, M. Tavernier, and A. Touati, Phys. Fenn. 9 S1, 409 (1974).